

# Third order elastic constants of semi-continuous casting ingot A3004 aluminum alloy and measurement of stress

Sennosuke Takahashi · Kiyoko Takahashi

Received: 19 September 2002 / Accepted: 11 April 2006 / Published online: 15 February 2007  
© Springer Science+Business Media, LLC 2007

**Abstract** The object of this study is measurement of a stress and the reliable third order elastic constants of the engineering material using the original theory and the measurement of elastic wave propagating velocity. The change of elastic wave propagating velocity caused by applied stress was measured for the specimen cut off from semi-continuous casting ingot of A3004 aluminum alloy. From the point of view of Lagrangian description where state before deformation was used as the reference coordinate, Murnaghan's third order elastic constants could be obtained by use of the changing ratio of elastic wave velocity under applied stress, stress–strain relation, and the equation of stress dependence on elastic wave velocity. As a result, authors found a new method of stress measurement by introducing the stress dependent coefficients to elastic wave velocity.

## Introduction

The studies on the measurement of third order elastic (TOE) constants for engineering materials have been carried out by Hughes and Kelly [1], Egle and Bray [2], Takahashi and Motegi [3] and so on. This experiment was performed considering the possibility of in situ measurement of stress for engineering products and construction materials in future and a theoretical

meaning was given to the stress measurement method. The Murnaghan's TOE constants and their measurement process on the semi-continuous casting aluminum alloy A3004 were reported in this paper.

## Experiments

### Sampling and test specimen

The A3004 Al alloy shows excellent ductility and is used as engineering material for processed goods. Table 1 shows the chemical composition of the sample alloy. Dimension of semi-continuous casting ingot and cutting position for sampling is shown in Fig. 1. The sample was cut off at 10 mm inner from the surface of ingot.

From the microstructure of sample, it was recognized that the sampling region was almost isotropic and the grain sizes were under 100  $\mu\text{m}$  in average as shown in Fig. 2.

The long (130 mm) and short (90 mm) test specimens which had identical grip length (30 mm) and cross-section of gauge region ( $20 \times 20 \text{ mm}^2$ ) but different gauge length were machined from the sample to eliminate unknown effect caused by the grip part. The test specimen adhered with transducer and strain gauge were shown in Fig. 3.

### Measurement system

Change of the elastic wave propagating velocity (time of flight) due to applied stress have to be precisely measured in order to obtain TOE constants of the sample. MBS-8000 ultrasonic measurement system of

S. Takahashi (✉) · K. Takahashi  
National Research Institute for Metals, 1321-15 Kanamori,  
Machida-shi, Tokyo 194-0012, Japan  
e-mail: fwnk4784@mb.infoweb.ne.jp

**Table 1** Chemical composition of A3004 sample (mass%)

Mn	Mg	Cu	Fe	Si	Zn	Cr	Ti	Al
1.09	1.27	0.23	0.40	0.28	0.07	0.03	0.03	Bal

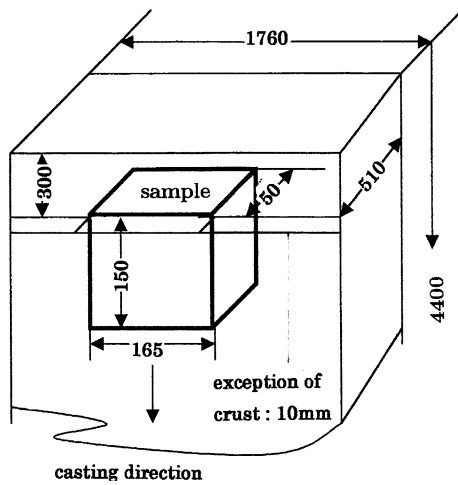


**Fig. 1** Sampling from semi-continuous casting ingot

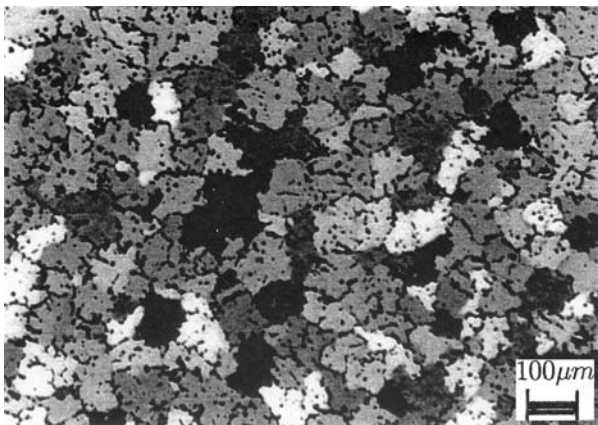


**Fig. 2** Microstructure of sample

MATEC Instruments Inc. was used to measure the time of flight. The piezoelectrical resonator of PZT type, a plate of  $10 \times 10 \text{ mm}^2$  was used as a transducer for longitudinal and transverse waves. The schematic diagram and overview of MBS-8000 ultrasonic measurement system is shown in Fig. 4. An Instron type tensile testing machine, a computerized strain measurement apparatus were used. The cross-head speed of testing machine was held constant at 0.02 mm/min and kept 5 min on the each load. The load cell used for measurement of stress was compensated by the standard gauge. The strain of specimens was measured by strain gauge adhered on the both sides of gauge region.

Measurement and calculation

As shown in Fig. 3, the test specimen adhered with transducers and strain gauge was installed in the Instron type tensile testing machine with specially designed chucks. Each result was automatically read out as shown in Fig. 4. Time of flight were measured under the static state of applied stress in the region from 0 MPa to 2.5 MPa. Adjacent temperature of the specimen and measuring device was kept constant at 24 °C. Measurement of time of flight was carried out by the following process; an elastic wave pulse was introduced into one end of a specimen, then the first and the second echoes were received by measuring device and time lag in these two echoes was digitized after statistical calculation by a computer. It was repeated 250 times a measurement under an unidirectional tensile stress  $\sigma_{11}$  and obtained five data were further averaged. In this case the elastic wave propagating velocity  $V_{ij}$  can be written as [3]

$$V_{ij} = V_o \left( 1 + \alpha_{ij} \cdot \frac{\sigma_{11}}{E} \right) \tag{1}$$

The first number in subscript of  $V$  indicates the propagating direction and second one the polarization direction.  $V_o$  is elastic wave propagating velocity at stress free. When the elastic wave propagates along the tensile stress direction (pass through grip’s region), stress dependent coefficients for elastic wave velocity  $\alpha_{ij}$  can be given as

$$\alpha_{ij} = 1 - \frac{E}{\sigma_{11}} \left[ \frac{L_b}{\Delta L} \left( \frac{\Delta t_b}{t_{ob}} \right) - \frac{L_a}{\Delta L} \left( \frac{\Delta t_a}{t_{oa}} \right) \right] \tag{2}$$

where  $E$  is Young’s modulus,  $L_a$  and  $L_b$  are total length of short and long specimens,  $\Delta L = L_b - L_a$ , subscript  $a$  and  $b$  denote short and long specimens,  $t_o$  is time of flight at stress free, then  $t_{oa} = L_a/V_{oa}$ ,  $t_{ob} = L_b/V_{ob}$ ,  $\Delta t_a = t_a - t_{oa}$ ,  $\Delta t_b = t_b - t_{ob}$ .  $t_a$  and  $t_b$  are time of flight of short and long specimens, respectively.

In the case of elastic wave pulse along the direction perpendicular to the tensile axis of specimen (not pass through grip’s region),  $\alpha_{ij}$  is given as

$$\alpha_{ij} = -\nu - \frac{E}{\sigma_{11}} \left( \frac{\Delta t_{ij}}{t_o} \right) \tag{3}$$

where  $\nu$  is Poisson’s ratio. The stress dependent coefficient  $\alpha_{ij}$  in Eq. 1 is obtained from Eq. 2 or 3 using the measured data.

**Fig. 3** Arrangement of sensors,  $E_t, E_l$ ; strain gauge of  $X_1$ , and  $X_2$  direction,  $L_{11}, L_{22}$ ; longitudinal wave transducer of  $X_1$  and  $X_2$  direction,  $S_{12}, S_{21}$ ; transverse wave transducer

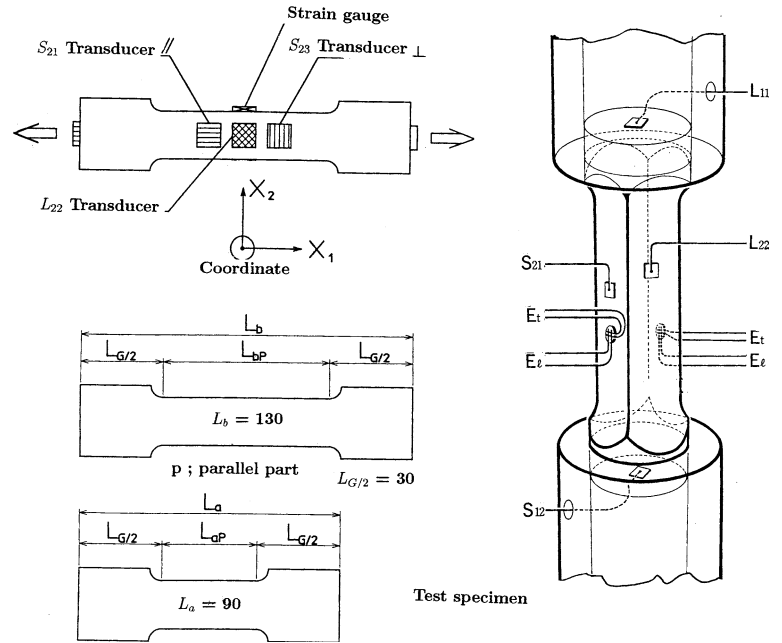
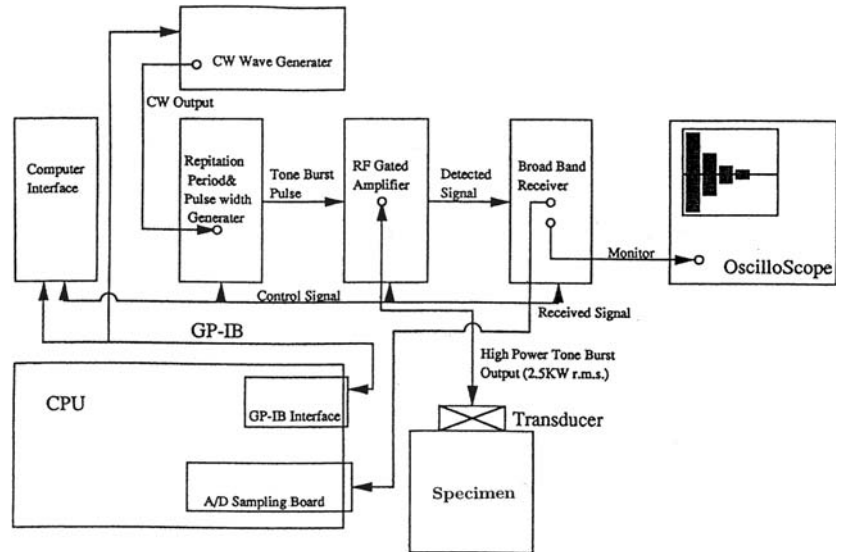


**Fig. 4** Schematic diagram of measurement system



When the elastic wave propagates and polarizes to  $X_1$  axis direction (the direction of applied stress  $\sigma_{11}$ ), the longitudinal wave velocity  $V_{11}$  is

$$\rho_o V_{11}^2 = \lambda + 2\mu + \frac{\sigma_{11}}{E} [5\lambda + 10\mu + 2(\ell + 2m) - 2\nu(\lambda + 2\ell)] \quad (4)$$

and the longitudinal wave velocity  $V_{22}$  propagating and polarizing vertically to tensile axis  $X_1$  is also given as follows [1]

$$\rho_o V_{22}^2 = \lambda + 2\mu + \frac{\sigma_{11}}{E} [\lambda + 2\ell - \nu(6\lambda + 10\mu + 4\ell + 4m)] \quad (5)$$

Setting  $i = 1, j = 1$  in Eq. 2, and from Eqs. 1 and 4, we obtain

$$\alpha_{11} = \frac{1}{2(\lambda + 2\mu)} [5\lambda + 10\mu + 2\ell + 4m - 2\nu(\lambda + 2\ell)] \quad (6)$$

Similarly setting  $i = 2, j = 2$  in Eq. 3, and from Eqs. 1 and 5, we obtain

$$\alpha_{22} = \frac{1}{2(\lambda + 2\mu)} [\lambda + 2\ell - \nu(6\lambda + 10\mu + 4\ell + 4m)] \quad (7)$$

where values of  $\alpha_{11}$  and  $\alpha_{22}$  are obtained from measured data, and  $\lambda$  and  $\mu$  are Lamè's constants,  $\ell$ ,  $m$  and  $n$  are Murnaghan's TOE constants.

From Eqs. 6 and 7, TOE constants can be given as follows

$$\ell = \frac{(2\alpha_{11} - 5)(\lambda + 2\mu)}{2(1 - 2\nu)} - \frac{2m - \nu\lambda}{(1 - 2\nu)}, \tag{8}$$

$$m = \left( \frac{\alpha_{11} - \alpha_{22}}{2(1 + \nu)} - 1 \right) (\lambda + 2\mu) - \frac{\mu}{2}$$

The transverse wave velocity  $V_{12}$ ,  $V_{21}$  and  $V_{23}$  are as follows [1]

$$\rho_o V_{12}^2 = \mu + \frac{\sigma_{11}}{E} \left[ \lambda + 4\mu + m - 2\nu(\lambda + \mu + m - \frac{n_{12}}{4}) \right],$$

$$\rho_o V_{21}^2 = \mu + \frac{\sigma_{11}}{E} \left[ \lambda + 2\mu + m - 2\nu(\lambda + 2\mu + m - \frac{n_{21}}{4}) \right],$$

$$\rho_o V_{23}^2 = \mu + \frac{\sigma_{11}}{E} \left[ \lambda + m - 2\nu(\lambda + 3\mu + m) - \frac{n_{23}}{2} \right]$$

Using  $\alpha_{12}$ ,  $\alpha_{21}$  or  $\alpha_{23}$  and the formula of  $V_{12}$ ,  $V_{21}$  or  $V_{23}$

$$n_{12} = \frac{2}{\nu} [ -(\lambda + 4\mu + m) + 2\nu(\lambda + \mu + m) + 2\mu\alpha_{12} ],$$

$$n_{21} = \frac{2}{\nu} [ -(\lambda + 2\mu + m) + 2\nu(\lambda + 2\mu + m) + 2\mu\alpha_{21} ],$$

$$n_{23} = 2 [ \lambda + m - 2\nu(\lambda + 3\mu + m) - 2\mu\alpha_{23} ]$$

where  $n_{12} = n_{21}$  is defined in the isotropic solid but it is difficult to obtain such equivalent relation to the measured values.

**Fig. 5** Time of flight vs. stress for longitudinal wave in the  $X_1$  axis of short specimen

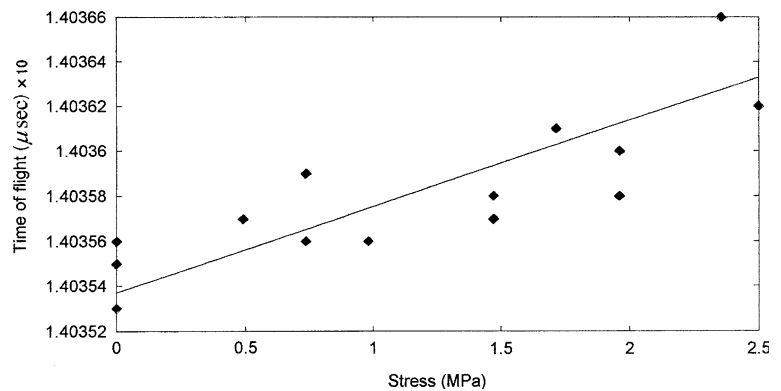
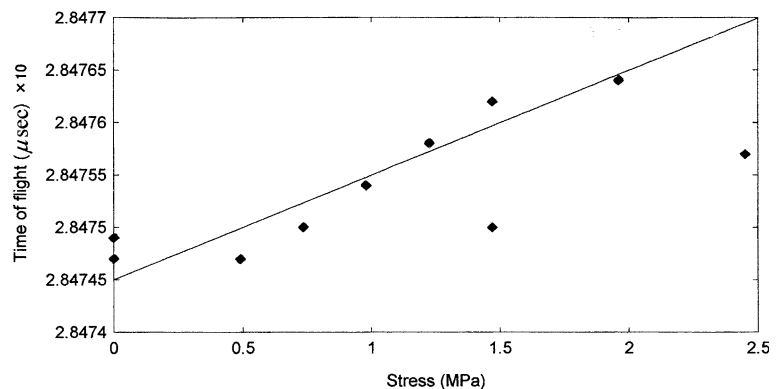


**Fig. 6** Time of flight vs. stress for transverse wave in the  $X_1$  axis of short specimen



**Experimental results**

The relation between time of flight and stresses was shown in Fig. 5 for longitudinal wave and in Fig. 6 for transverse wave.

Longitudinal wave velocity  $V_o$  and transverse wave velocity  $V'_o$  at nonapplied stress are

$$\rho_o V_o^2 = \lambda + 2\mu, \quad \rho_o V_o'^2 = \mu, \tag{9}$$

$$\frac{\lambda}{\mu} = \frac{2\nu}{1 - 2\nu} = \frac{\rho_o(V_o^2 - 2V_o'^2)}{\rho_o V_o'^2}$$

where  $\rho_o$  is density of specimen at nonapplied stress.

From average of measured data as shown in Figs. 5 and 6,  $V_o$  and  $V'_o$  at nonapplied stress were obtained as  $V_o = 6409.3$  m/s,  $V'_o = 3160.7$  m/s. Using  $\rho_o = 2.719$  g/m<sup>3</sup>.

$\lambda/\mu = 2.078$ , Lamè’s constants  $\lambda$ ,  $\mu$  and  $\nu$  can be obtained from Eq. 9. Similarly these values can be given from stress–strain diagram.  $\lambda$ ,  $\mu$  and  $\nu$  obtained by both ways were shown in Table 2. Stress dependent coefficient of elastic wave velocity  $\alpha_{ij}$  is shown in Table 3. The TOE constants of A3004 Al alloy derived from above data are shown in Table 4. Figure 7 shows

**Table 2** Lamè’s constants, Young’s modulus ( $\times 10^3$  MPa) and Poisson’s ratio

Method	$\lambda$	$\mu$	$E$	$\nu$
Elastic wave	56.26	26.64	71.35	0.339
Stress–strain	55.42	26.66	71.32	0.338

**Table 3** Stress dependent coefficients  $\alpha_{ij}$

$\alpha_{11}$	$\alpha_{22}$	$\alpha_{12}$	$\alpha_{21}$	$\alpha_{23}$
-0.247	2.943	-0.529	-1.857	2.041

**Table 4** TOE constants of A3004 alloy,  $\times 10^3$  MPa

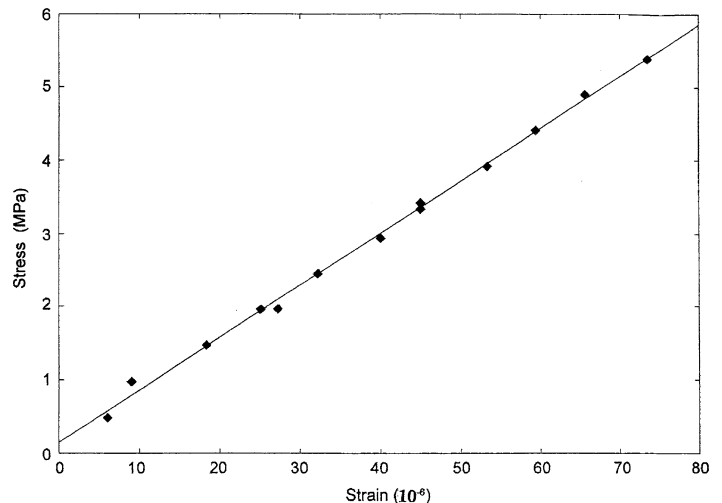
$\ell$	$m$	$n_{12}$	$n_{21}$	$n_{23}$
564.63	-231.69	-353.64	-350.25	-440.16

the stress–strain curve obtained by the experiment. The nonlinear equation in the uniaxial tensile test situation can be described as follows

$$\sigma_{11} = E\eta_{11} + [E + \ell(1 - 2\nu)^2 + 2m(1 - \nu^2)]\eta_{11}^2 \quad (10)$$

Setting the strain  $\eta_{11}$  at  $70 \times 10^{-6}$  and using the data in Table 2, the values of stress were about 5 MPa for 1st term only and about 4.997 MPa from a calculation included the 2nd term in Eq. 10. In Eq. 10, 1st term is composed of the Hook’s law and the 2nd one is nonlinear system. Namely Eq. 10 shows mathematically nonlinear system, but the curvature of stress–strain diagram is extremely small.

**Fig. 7** Stress–strain relation of A3004 Al alloy



**Considerations**

Using the change of longitudinal wave velocity  $\Delta V_{11}$  or changing ratio of time of flight  $\Delta t_{11}/t_0$  along the direction parallel to applied stress  $\sigma_{11}$ , the measured  $\alpha_{11}$ , and Eq. 1, we can obtain the value of applied stress  $\sigma_{11}$  as follows

$$\sigma_{11} = \frac{E \Delta V_{11}}{\alpha_{11} V_0} = \frac{E}{(1 - \alpha_{11})} \frac{\Delta t_{11}}{t_0} \quad (11)$$

Similarly from the change of wave velocity  $\Delta V_{22}$  or time of flight  $\Delta t_{22}/t_0$  along the direction perpendicular to applied stress  $\sigma_{11}$  and  $\alpha_{22}$ , we can also obtain the value of applied stress  $\sigma_{11}$  as follows

$$\sigma_{11} = \frac{E \Delta V_{22}}{\alpha_{22} V_0} = -\frac{E}{(\nu + \alpha_{22})} \frac{\Delta t_{22}}{t_0} \quad (12)$$

where  $\alpha_{11}$  and  $\alpha_{22}$  are the stress dependent coefficients of measurable values and constituted of Lamè’s and TOE constants.

Above equations can be applicable for the measurement of stress of other engineering materials, and supported by the third order elastic theory.

The attention was specially payed to sampling from semi-continuous casting ingot, but there was a difference between measured values  $n_{21}$  and  $n_{23}$ . The similar difference were also shown in the other experiments performed for samples prepared as isotropic material. The preparation of isotropic material is technically difficult from the point of view of evaluation on the value of  $n_{ij}$ .

Change of time of flight with stress could be observed at near five figures in micro-second, therefore the measurement values sensitively fluctuated with the state of interface between transducer and specimen, wiring of devices, quality of transducer, sampling of pulse echoes into gates in the computer display, and room temperature and so on.

### Conclusions

1. A change of the elastic wave propagating velocity due to static applied stresses was measured for the specimen cut off from the semi-continuous casting ingot of A3004 aluminum alloy.
2. The Murnaghan's third order elastic constants  $\ell$ ,  $m$ ,  $n$ , Lamè's constants and Poisson's ratio could be obtained for the engineering material using measurement values related to stress dependence of elastic wave velocity.
3. A theoretical support was given to the measuring method of stress and the change of the elastic wave

velocity owing to applied stress, so this method can be practically and effectively applied to the construction materials by use of high precision instruments and technique.

4. The equation of the nonlinear stress-strain relation was introduced in the uniaxial stress situation and the stress calculated from nonlinear equation was compared with the stress measured under linear process.

**Acknowledgements** The authors hereby express their heartfelt thanks to Dr. Kazuhiko Seki, Senior Research Scientist of National Institute of Advanced Industrial Science and Technology for his help.

### References

1. Huges DS, Kelly JL (1953) Phys Rev 92(5):1145
2. Egle DM, Bray DE (1978) Report No. FRA/ORD-77/34.1, U.S. Depart. of Transp. F.R.A. Jan
3. Takahashi S, Motegi R (1987) J Mater Sci 22:1857